[CANCER RESEARCH 63, 4677–4683, August 1, 2003]

Lsh-deficient Murine Embryonal Fibroblasts Show Reduced Proliferation with Signs of Abnormal Mitosis[1]

Tao Fan, Qingsheng Yan, Jiaqiang Huang, Sharon Austin, Edward Cho, Doug Ferris, and Kathrin Muegge[2]

Laboratory of Molecular Immunoregulation [T. F., Q. Y., J. H., K. M.], Laboratory of Leukocyte Biology [S. A., D. F.], Image Analysis Laboratory [E. C.], and Basic Research Program [S. A., E. C., D. F., K. M.], Science Applications International Corporation-Frederick, Inc., National Cancer Institute Frederick, Frederick, Maryland 21702-1201

ABSTRACT

Genomic hypomethylation and chromosomal instability are frequent characteristics of human cancer cells. Targeted deletion of *Lsh* leads to a global defect in genomic methylation, and *Lsh*-deficient mice die at birth with a reduced body weight. Here, we examine the growth pattern of embryonal fibroblasts derived from $Lsh^{-/-}$ mice. The absence of Lsh leads to a severe proliferative defect of fibroblasts with lower saturation density, early signs of senescence, and a lower frequency of immortalization. The impaired growth rate *in vitro* may be in part responsible for the small size of Lsh-deficient mice. In addition, $Lsh^{-/-}$ fibroblasts accumulated high centrosome numbers, formed multipolar spindles, displayed micronuclei formation, and elevated nuclear DNA content. A similar increase in centrosome abnormalities was observed when wild-type fibroblasts were treated with a DNA-demethylating agent, suggesting that genomic hypomethylation plays an important role in mitotic defects of $Lsh^{-/-}$ murine embryonal fibroblasts, possibly by altering chromatin structure. Because supernumerary centrosomes are a common feature in cancer cells, this Lsh-dependent pathway has the potential to contribute to genetic instability and chromosomal aberrations during tumor progression.

INTRODUCTION

Epigenetic changes are important for embryonic development, aging, and tumorigenesis. CpG methylation is a major mechanism of epigenesis and is involved in X-inactivation, imprinting, and silencing of tumor suppressor genes (1). Methylation is thought to repress transcription via recruitment of methyl-DNA binding proteins and histone deacetylases rendering chromatin inaccessible. Aberrant methylation patterns are frequently associated with cancer development (2–4). Many solid tumors show global hypomethylation and simultaneously hypermethylation of tumor suppressor genes. Although Dnmts[3] have been identified, how Dnmts are targeted to specific genomic sites and how aberrant methylation patterns arise in cancer cells is unclear.

Recently, members of the SNF2 family have been implicated in regulating genomic methylation (5). SNF2 members often participate in larger multiprotein complexes (*e.g.*, the SWI/SNF chromatin remodeling complex) that are able to disrupt histone DNA interactions (6). Mutations of SNF2 homologues (such as ATRX, Lsh, and DDM1) have been reported to alter methylation levels. The *ATRX* gene is responsible for a number of human X-linked mental retardation syndromes. Upon mutation of *ATRX*, genomic DNA shows changes in methylation patterns of some repeated sequences such as ribosomal DNA arrays (7). *DDM1* mutations in *Arabidopsis thaliana* give rise to a global genomic methylation defect (8). Another SWI/SNF member, Lsh (lymphoid-specific helicase), is a key modulator of CpG methylation in mice (9, 10). A human Lsh homologue, proliferation-associated SNF2-like gene, has been recently cloned from leukemia cells (11). Targeted deletion of murine *Lsh* leads to a reduction of global genomic methylation to 30–50% of wild-type methylation levels (12, 13). The presumed chromatin remodeling activity of ATRX, DDM1, or Lsh suggests that chromatin structure, in part, determines genomic methylation patterns. Posttranslational modifications of histone tails such as acetylation and methylation are also implicated in the mechanisms of CpG methylation (14, 15).

Lsh-deficient mice show multiple developmental defects, indicating that Lsh is crucial for normal development (12, 13, 16). Loss of functional Lsh leads to death of newborns, to renal and hematopoietic defects with reduced lymphoid development, and a failure of lymphoid cells to proliferate *in vitro*. Early death of $Lsh^{-/-}$ mice is accompanied by signs of reduced growth with a birth weight of 80% of that of wild-type controls. Here, we assess the proliferative capacity of embryonal fibroblasts derived from $Lsh^{-/-}$ mice. We report a severe growth defect of $Lsh^{-/-}$ MEFs. In addition, cells show signs of abnormal mitosis with centrosome amplification and multipolar spindle formation. Similarly, DNA hypomethylation caused by 5-aza-dC treatment increased centrosome numbers in wild-type MEF cultures. These results support a model in which Lsh, a regulator of genomic methylation and normal chromatin structure, is also important for normal cell cycle division. Because centrosomes are important for bipolar spindle formation to ensure equal segregation of chromosomes to daughter cells (17–19), these findings suggest a potential role for Lsh in protecting chromosomal stability.

MATERIALS AND METHODS

Cell Culture. Embryos from crosses between $Lsh^{+/-}$ mice were removed at day 13.5 of gestation and genotyped by PCR as described before (12). Animal care was provided in accordance with the procedures outlined in the "Guide for the Care and Use of Laboratory Animals." The embryos were washed twice with PBS under sterile conditions, and embryonic tissues were finely minced and digested by incubation in 0.25% trypsin-EDTA solution (Life Technologies, Inc.) for 15 min at 37°C. The cells of the resulting suspension were plated onto 10-cm dishes. Primary mouse fibroblast cells were grown in DMEM supplemented with 10% heat-inactivated fetal bovine serum (Hyclone), 2 mM L-glutamine, 100 units/ml penicillin, and 100 μg/ml streptomycin. After 2 days, cells were split (termed passage one) and consecutively split every third day. For analysis of growth curves, cells were trypsinized and diluted to 3×10^4 cells/ml, seeded in replicate 24-well plates with 1-ml cell suspension/well. Every 24 h, the cells were trypsinized and counted for 8 consecutive days. For calculation of population doubling and for generation of immortalized cells, serial cultures were performed according to the 3T3 or 3T9 protocol (20). Briefly, 3×10^5 (3T3) or 9×10^5 (3T9) cells were plated on 6-cm dishes. Every 3 days, cells were trypsinized, counted, and replated at starting densities. DNA synthesis was determined by [^{3}H]thymidine incorporation. Cells were seeded at 3×10^3 cells/well in triplicate into 96-well microtiter plates and cultured for 24 h, then cells were pulsed with 5 μCi/ml of methyl-[^{3}H]thymidine (2 Ci/mmol; Amersham) for 20 h. Cells were trypsinized, and the incorporation of radioactivity into DNA was measured by a liquid scintillation counter. For colony formation efficiency, 1×10^4 cells

Received 12/26/02; accepted 5/30/03.

The costs of publication of this article were defrayed in part by the payment of page charges. This article must therefore be hereby marked *advertisement* in accordance with 18 U.S.C. Section 1734 solely to indicate this fact.

[1] This project has been funded in whole or part with federal funds from the National Cancer Institute, NIH, under Grant No. N01-C0-12400.

[2] To whom requests for reprints should be addressed, at Laboratory of Molecular Immunoregulation, Basic Research Program, SAIC-Frederick, National Cancer Institute, Building 469, Room 243, Frederick, MD 21701-1201. Phone: (301) 846-1386; Fax: (301) 846-7077; E-mail: Muegge@ncifcrf.gov.

[3] The abbreviations used are: Dnmt, DNA methyltransferase; SNF, sucrose nonfermenting; BrdUrd, bromodeoxyuridine; MEF, murine embryonal fibroblast; 5-aza-dC, 5-aza-2′-deoxycytidine; DAPI, 4′,6-diamidino-2-phenylindole; Cdk2, cyclin-dependent kinase 2.

were distributed on 10-cm dishes and incubated with regular changes of medium every 3 days. After 2 weeks of incubation, dishes were fixed in 95% methanol/5% PBS for 10 min at 4°C and stained with Giemsa. The number of visible colonies (>50 cells) was scored. For demethylation, cells were cultured in media containing 2.5 μM 5-aza-dC (Sigma). The medium was changed every 24 h with media containing fresh 5-aza-dC for 4 days. The cells were fixed with methanol/acetone and stained with anti-γ tubulin and antipericentrin antibodies, or DNA was extracted and examined for CpG hypomethylation at minor satellite repeats using Southern analysis (13).

SV40 Large T Antigen Transfection. MEFs were seeded at the concentration of 1.5×10^5 in 10-cm dishes 15 h before transfection. Cells were cotransfected with 2.5 μg of SV40 DNA and 0.5 μg of pcDNA3 as a selectable marker using the Lipofectin kit. The cells were selected with 40 μg/ml hygromycin for wild-type and heterozygous cells and 20 μg/ml for $Lsh^{-/-}$ cells 48 h after transfection, and hygromycin containing culture media was changed every third day. After 14 days of selection, the selected cells were washed with PBS and fixed in 95% methanol/5% PBS for 10 min at 4°C, stained with Giemsa, and colony numbers were counted.

Cell Cycle Analysis. To generate immortalized cells MEFs were cultured according to the 3T9 protocol. MEFs were trypsinized at different passages, seeded at 3×10^5/6-cm dish and harvested 24 h later for cell cycle analysis. Cell suspensions were washed twice in PBS and fixed with cold 70% ethanol for 4 h. After fixation, cells were washed once with PBS, then stained in 25 μg/ml propidium iodide (Sigma) with 100 μg/ml RNase A in PBS. Flow cytometry analysis was performed on a Coulter Epics XL-MCL cytometer. The data were collected and analyzed using the Coulter System II software provided by the manufacturer.

Indirect Immunofluorescence. Cells were seeded on coverslips and incubated for 24 h, then washed twice with PBS and fixed with 50% methanol/50% acetone for 5 min at −20°C. Cells were probed overnight at 4°C with primary antibodies as follows: α-tubulin (1:300, mouse IgG1; Sigma); γ-tubulin (1:6000, mouse IgG1; Sigma); and pericentrin 4B (1:300, rabbit polyclonal; PKL). Antibody-antigen complexes were detected by incubation for 1 h at room temperature with rhodamine or FITC-conjugated secondary antibodies. Samples were washed three times with PBS and then counterstained with DAPI. The cells were observed under a fluorescent microscope (Zeiss) or by three-dimensional confocal microscopy (LSM 310 confocal microscope; Carl Zeiss, Inc., Thornwood, NY). For DNA content analysis, subconfluent MEFs were labeled with the fluorescent DNA dye, DAPI, and imaged with three-dimensional confocal microscopy set up to ensure no saturation of pixels. Images were then analyzed using the MIPAV image analysis software (21). Individual nuclei (~40–50) were segmented from the three-dimensional images by a threshold operation, and the resulting mask was used to calculate the total fluorescence signal for each nuclei. After the background signal was subtracted, the net signal for each individual nuclei was proportional to the DNA content.

BrdUrd Incorporation Assay. The BrdUrd incorporation assay was performed using the BrdUrd labeling and detection kit (Roche Molecular Biochemicals) according to the manufacturer's instructions. Briefly, cells were seeded on coverslips and cultured for 24 h. After incubation for 2 h in media containing BrdUrd, cells were fixed in ethanol fixative [70% ethanol in 50 mM glycine (pH 2.0)] for 20 min at −20°C and then probed with antipericentrin polyclonal and anti-BrdUrd monoclonal antibodies for 30 min at 37°C. Antigen-antibody complexes were detected by FITC-conjugated sheep antimouse IgG and rhodamine-conjugated goat antirabbit IgG antibodies. BrdUrd incorporation rate of the whole population and the number of centrosomes/BrdUrd-positive cell were scored.

Western Analysis. Proteins were extracted from MEFs as described previously (16). Twenty μg of nuclear protein extract were separated on an 8% Tris-glycine SDS-polyacrylamide gel by electrophoresis and blotted onto nitrocellulose. The following antibodies were used for detection of cell cycle proteins: p21 (no. 556430), P53 (no. 554164), and p27 (no. 554069) are from PharMingen; and cyclin E (no. sc-481) and cdk2 (no. sc298) are from Santa Cruz Biotechnology. After incubation with secondary horseradish peroxidase-coupled antibodies (Amersham Pharmacia), detection of horseradish peroxidase was performed using the enhanced chemiluminescence Western blotting detection reagents according to the manufacturer's instructions and visualized on Hyperfilm ECL chemiluminescent film.

RESULTS

Reduced Growth Rate of $Lsh^{-/-}$ Embryonal Fibroblasts in Culture. Lsh-depleted lymphocytes fail to proliferate *in vitro*, and Lsh-deficient mice are smaller in size than their littermates possibly because of a reduced growth rate (12, 16). Thus, we examined the growth property of embryonal fibroblast (MEF) cells derived from $Lsh^{-/-}$ embryos. MEFs derived from embryos of day 13.5 of gestation were seeded at equal densities and their cell numbers monitored daily. As shown in Fig. 1*A*, $Lsh^{-/-}$ MEFs accumulate at lower cell numbers in culture with roughly half the number compared with that of heterozygous and wild-type cultures. The saturation density of $Lsh^{-/-}$ MEFs was considerably lower then those of wild-type cells or heterozygous cells. When MEFs were passaged every third day and cultured at low cell density according to the 3T3 protocol, wild-type

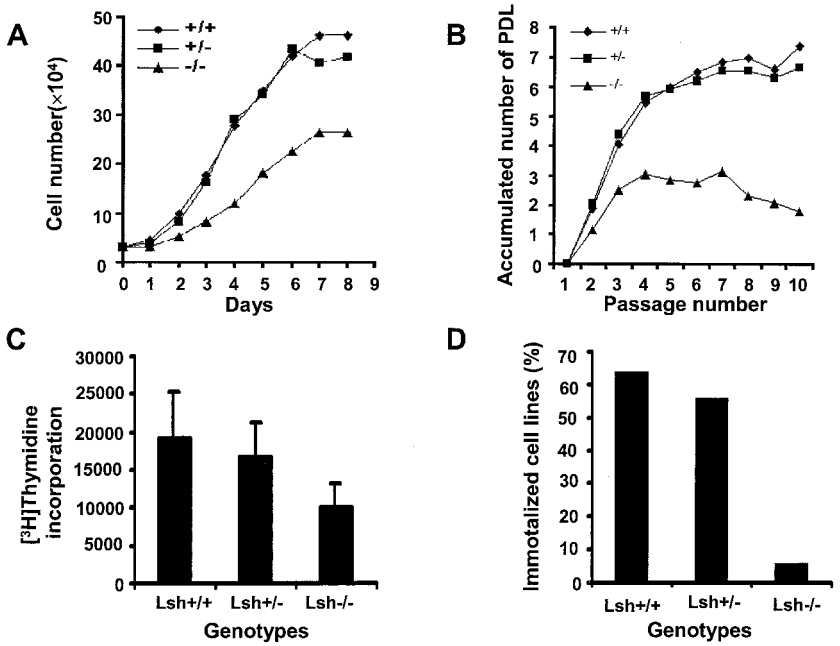

Fig. 1. Reduced growth rate of $Lsh^{-/-}$ MEFs. *A*, Growth curve. MEFs were seeded on 24-well plate at the concentration of 3×10^4 and counted daily. Each data point represents the mean of three experiments. *B*, population doubling. Cells were cultured according to the 3T3 protocol. *C*, DNA synthesis. Replication of MEFs was measured by thymidine incorporation for 24 h. Values shown represent the average of three independent experiments. *D*, immortalized cell lines. MEFs were cultured according to the 3T3 protocol. Independent cell cultures that started growing after senescence were counted.

Table 1 *Reduced colony formation efficiency in $Lsh^{-/-}$ MEFs*

Genotypes	(Colonies/1 × 10^4 cells/10-cm dish)		
	$Lsh^{+/+}$	$Lsh^{+/-}$	$Lsh^{-/-}$
Expt. 1	6,18,29,33	4,5,8,9,12,14	0,2,2,2,3,6,16,21
Expt. 2	8,21,32,34	2,6,49	0,0,0,0,1,3
Expt. 3	18,31,37,120	2,18,101	0,0,0,1,3,8
Expt. 4	20,31,34	10,73	0,0,0,0,3,6,7
Expt. 5	10,28,35,56,102	12,15,79,86,98	0,1,2,5,7
Average	35.15	31.74	3.09

Table 2 *Reduced colony formation after SV40 large T antigen transfection*

	$Lsh^{+/+}$	$Lsh^{+/-}$	$Lsh^{-/-}$
Expt. 1	48,59,64	35,75	6,6,7
Expt. 2	7,51,58,71,110	9,46,68,81,85	0,0,7,9,35
Expt. 3	70,75,116	31,41,70	8,24
Average	66.3	54.1	10.2

and heterozygous MEFs grow with a cell doubling time of ~1.5 days (Fig. 1*B*). In contrast, $Lsh^{-/-}$ MEFs show significantly lower proliferative capacity with a doubling time of ~3 days. The observed lower cell numbers in Lsh-deficient MEFs could be caused by a reduced growth rate or alternatively could be because of an enhanced death rate. However, there was no evidence for enhanced cell death in the absence of Lsh, as measured by trypan blue exclusion or by assessing apoptotic rates [by terminal deoxynucleotidyl transferase-mediated nick end labeling assay, annexin stain, propidium iodide staining, or DNA fragmentation on gel electrophoresis (data not shown)]. Furthermore, incorporation of tritiated thymidine, indicative of DNA synthesis, was reduced to half of that of wild-type controls (Fig. 1*C*). This suggests that the growth rate of MEF cultures is reduced in the absence of Lsh.

Reduced Transformation rate in $Lsh^{-/-}$ Embryonal Fibroblasts. Primary cells have a limited life span in culture. Around passage 8–10 wild-type MEFs reach a plateau phase of growth and undergo replicative senescence (becoming larger, flat, and nonrefractile; Fig. 1*B*). $Lsh^{-/-}$ MEF cultures ceased growing two to three passages earlier than their wild-type littermates, and $Lsh^{-/-}$ cultures exhibited a higher percentage of giant senescent cells with large nuclei. Spontaneous escape from senescence occurs in wild-type cultures within 2 weeks of culture resulting in outgrowth of immortalized cell lines. In contrast, in $Lsh^{-/-}$ cultures, cell numbers declined, and in most cases, the cultures perished completely (Fig. 1*B*). Only 5% of $Lsh^{-/-}$ cultures derived from different embryos recovered from this senescence and established immortalized cell lines, whereas most wild-type cultures (63%) gained an immortal phenotype (with >50 passages; Fig. 1*D*). To quantify the spontaneous immortalization potential of $Lsh^{-/-}$ MEFs, a colony formation assay was used. When MEF cultures are plated at low density, a premature senescence program is induced, and the formation of visible colonies is correlated with their spontaneous escape of the senescence. As shown in Table 1, $Lsh^{-/-}$ MEFs formed few or no colonies (on average $3/10^4$ cells). This capacity is 10-fold lower than that of wild-type littermates (~$30/10^4$ cells). In addition, the size of the $Lsh^{-/-}$-derived colonies were much smaller than that of wild-type controls, indicating impaired growth. Thus, the lower colony formation capacity, together with the decreased ability to survive senescence, suggested a reduced immortalization rate in the absence of Lsh.

Transformation with the large T antigen of SV40 can overcome the senescence program and is sufficient to immortalize mouse embryonal fibroblasts. To test whether inactivation of the RB/p53 pathways can transform $Lsh^{-/-}$ MEF culture, Lsh-deficient cells were transfected with SV40 large T antigen. Both wild-type and Lsh-deficient cells were capable of forming colonies after SV40 transfection, indicating that MEFs can be transformed by the large T antigen of SV40 (Table 2). However, $Lsh^{-/-}$ cultures exhibited diminished colony formation efficiency in comparison with wild-type cultures (10.2 *versus* 66.6 colonies). Even if the decreased proliferative capacity of Lsh-deficient cells is taken into account and the numbers adjusted accordingly, Lsh-deficient MEFs are still reduced in their transformation efficiency to half of that of wild-type cells (an average of 33.8 colonies in $Lsh^{-/-}$ cultures *versus* 66.6). This indicates that neither the prolifer-

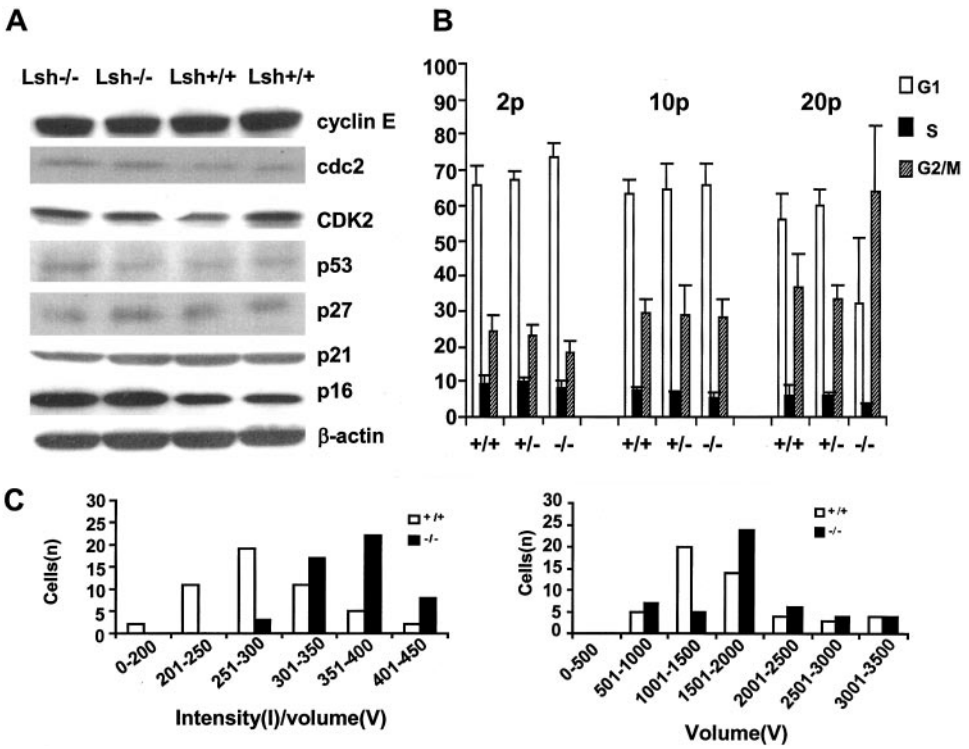

Fig. 2. Cell growth and cell cycle gene expression. *A*, expression of cell cycle regulatory proteins. Proteins were extracted from subconfluent MEF cultures and subjected to Western analysis using the indicated antibodies. *B*, cell cycle analysis at different MEF passages. MEFs from different culture passages were seeded at 3 × 10^5/6-cm dish. Cells were harvested after 24 h and stained with propidium iodide. The percentage of cells in each cell cycle stage was determined by flow cytometry. *C*, DNA content analysis. Immortalized wild-type and $Lsh^{-/-}$ MEFs were seeded on coverslips. After 24 h, cells were fixed and stained. The cell volume and DNA content were determined under the confocal microscope. *Left:* intensity/volume distribution. *Right:* cell volume distribution.

ative defect nor the reduced transformation efficiency caused by the loss of Lsh could be fully restored by inactivation of the p53/Rb pathways.

Cell Cycle Analysis. To investigate the mechanism of reduced cell proliferation in *Lsh*$^{-/-}$ MEFs, the expression of cell cycle proteins was analyzed. Cell lysates were prepared from asynchronous MEF cultures and subjected to immunoblot analysis and probed with different antibodies. There was no detectable change between Lsh-deficient or wild-type cells in protein expression levels for p21, p27, p53, and cyclin E (Fig. 2*A*) or cyclin A, cyclin D2, E2F2, and Rb (data not shown). A few Lsh$^{-/-}$-derived MEF cultures displayed a slight increase in p16 protein amounts that correlated with accelerated senescence (Fig. 2*A*; Ref. 22). Furthermore, some cultures showed slightly higher Cdc2 levels in comparison with littermate controls. Cdc2/cyclinB1 is crucial for entry into mitosis and the organization of centrosomes and microtubules. To test whether *Lsh*$^{-/-}$ cultures arrest during cell cycle progression, we examined the cell cycle stages by propidium iodide staining using flow cytometric analysis (Fig. 2*B*). Early passage cells (P2) displayed a slight increase (8%) in G_1 populations in the absence of Lsh, which may contribute but cannot fully explain the reduced growth capacity. At passage 10 (P10), both wild-type and Lsh-deficient cells had reached replicative arrest known as senescence and showed an overall reduction in the proportion of cells in S phase. There was no detectable difference in cell cycle distribution between different genotypes at P10. At passage 20, the proportion of *Lsh*$^{-/-}$ MEF cells with 4N was augmented, although wild-type MEFs also exhibited enhanced DNA content (63% in *Lsh*$^{-/-}$ *versus* 36% in wt). To measure the DNA content more accurately, confocal microscopy was used. Fig. 2*C* shows an enhanced proportion of cells in *Lsh*$^{-/-}$ cultures with higher fluorescence intensity/cell and larger volume/cell. Thus, the higher DNA content in Lsh-deficient MEFs in comparison with wild-type control cells could be indicative for an abnormal mitosis in Lsh-deficient cells leading to abnormal chromosome numbers.

Increased Centrosomes Numbers in *Lsh*$^{-/-}$ *MEFs*. Cancer cells frequently become polyploid because of defects in mitosis and failure to complete cytokinesis (17–19, 23–26). To examine whether Lsh-deficient MEFs had signs of abnormal mitosis, cultured cells were stained with anti-γ-tubulin and antipericentrin antibodies for detection of centrosomes (Fig. 3, *A* and *B*). Because murine MEFs have a tendency to accumulate centrosomes at later passages (27), we examined only early passages (P2–P4). Centrosomes are the primary microtubule organization center and play a dominant role in spindle formation. The fidelity of centrosome duplication once/cell cycle

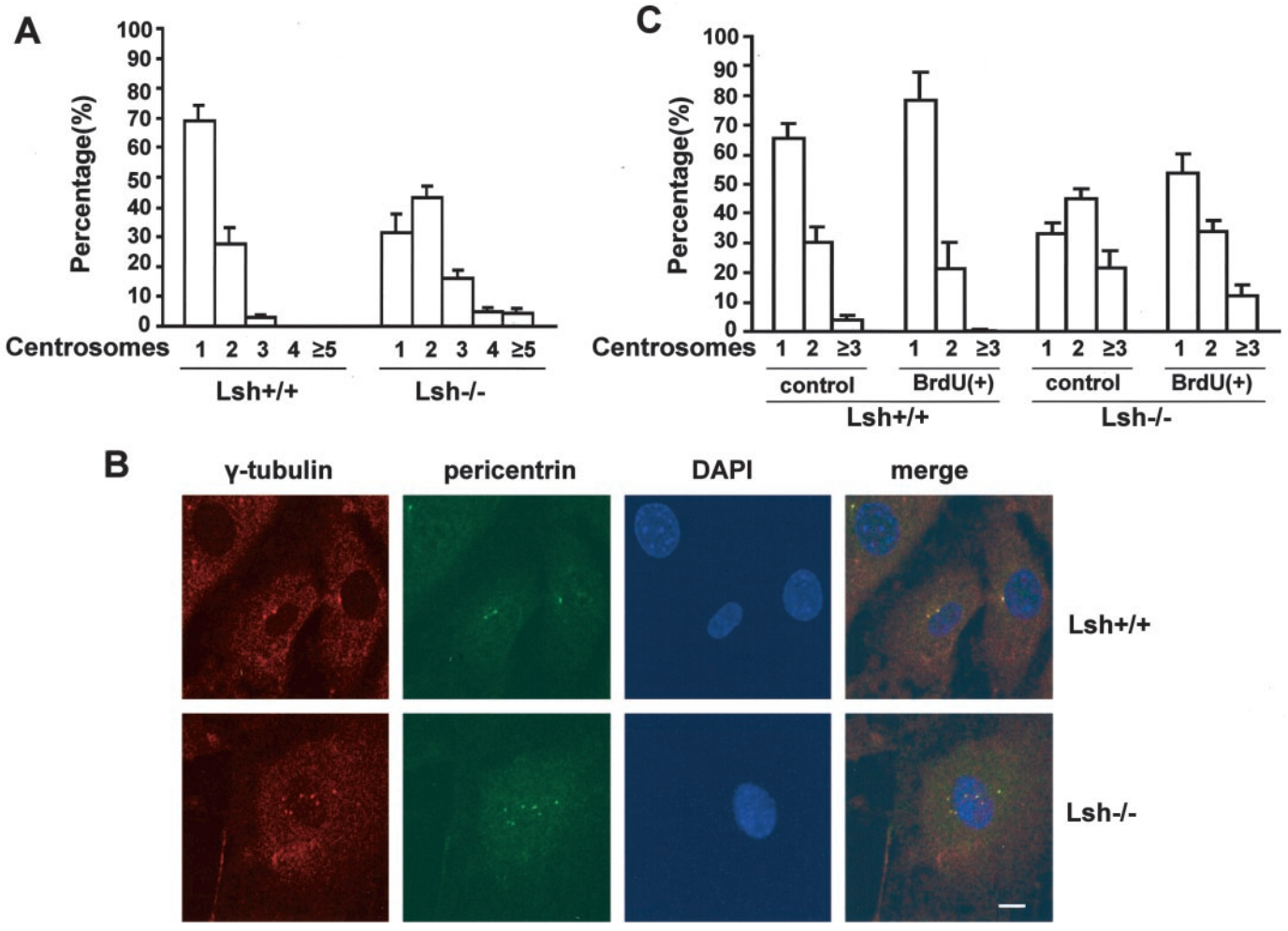

Fig. 3. Increase of centrosome numbers in *Lsh*$^{-/-}$ MEFs. *A*, MEFs at passage 2–4 were seeded on coverslips and stained with antipericentrin antibodies. The number of centrosomes/cell in at least 500 cells was evaluated in each experiment, and the *error bars* indicate the SD of three independent experiments *B*, MEFs at passage 2–4 were seeded on coverslips and costained with anti-γ-tubulin (rodamine-conjugated) and antipericentrin (FITC-conjugated) antibodies to detect centrosomes. Cells were then counterstained with DAPI for visualization of nuclei. *Scale bar*, 10 μm. *C*, reduced proliferation capacity in *Lsh*$^{-/-}$ MEFs with abnormal centrosome numbers. MEFs were costained with anti-BrdUrd (to detect entry into S phase) and antipericentrin antibodies (to detect centrosomes). Centrosomes were counted in the whole population and re-counted in BrdUrd-positive cells only. The number of centrosomes/cell in at least 500 cells was evaluated in each experiment, and the *error bars* indicate the SD from three independent experiments.

determines the number of spindle poles during mitosis and thus is important for balanced chromosomal transmissions to daughter cells. Most cells at early passages have only one centrosome (68% in wild-type; Fig. 3*A*). Centrosomes duplicate at the G_1-S-phase transition to ensure a bipolar spindle formation. Thus, a smaller fraction in wild-type cultures (~28%) show two centrosomes corresponding to the fraction of cells in S or later cell cycle phases (see fluorescence-activated cell sorting analysis in Fig. 2*B*). In contrast, in *Lsh*$^{-/-}$ MEFs, the proportion of cells with one centrosome *versus* two centrosomes was skewed (68 and 28% in wild-type *versus* 32 and 43% in *Lsh*$^{-/-}$ MEFs). Furthermore, *Lsh*$^{-/-}$ MEFs showed an increase in cells with abnormal centrosome numbers of three or more centrosomes (25 *versus* 4% in wild-type). Frequently, *Lsh*$^{-/-}$ MEF cultures showed very high numbers of centrosomes with up to 15 centrosomes (Fig. 3*B* for example shows seven centrosomes) that could not be observed in wild-type controls. Thus, Lsh-deficient MEFs show signs of aberrant mitotic events with increased centrosome numbers.

Abnormal Spindle Formation in the Absence of Lsh. Supernumerary centrosomes may nucleate multipolar spindles that could lead to unequal segregation of genetic material. Therefore, we next examined whether supernumerary centrosomes in Lsh-deleted MEFs were associated with defective spindle formation. MEFs were treated with nocadozole to enrich for mitotic cells and costained with α-tubulin and pericentrin to visualize the nucleated microtubule spindles and centrosomes. As shown in Fig. 4 many extra centrosomes in Lsh-deficient MEF cell cultures are functional and can form multipolar spindles leading to aberrant chromosomal distribution. However, aberrant spindle organization was not detectable in all cells with additional centrosomes numbers. For example, clustering of two or more centrosomes at one spindle pole was occasionally detected, resulting in a cell with a bipolar spindles. These cells may perform normal mitosis, despite their aberrant centrosome number (23–26). As additional evidence of abnormal spindle organization, we detected micronuclei formation indicative of lagging chromosomes in ~16% of *Lsh*$^{-/-}$ MEFs: spike formation, signs of nuclear splitting and separation of part of the nucleus leading to complete micronuclei (Fig. 5).

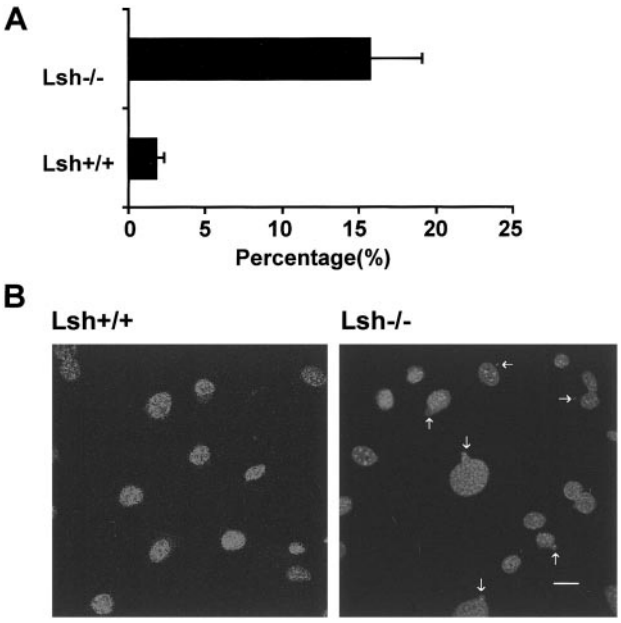

Fig. 5. Micronuclei formation in *Lsh*$^{-/-}$ MEFs. MEFs of Lsh-deficient mice at passage 4 were seeded on coverslips and stained with DAPI for detection of DNA content. *A*, scoring of cells with evidence of micronuclei. *B*, images of wild-type and Lsh-deficient cells. *Arrows* indicate different stages of micronuclei formation. *Scale bar*, 20 μM.

In contrast, micronuclei were barely detectable at early passage wild-type MEF cultures. Thus, deletion of Lsh leads to an increase in functional centrosome number, formation of multipolar spindles, and signs of unbalanced chromosome segregation.

Reduced Proliferative Capacity in *Lsh*$^{-/-}$ MEFs with Abnormal Amplified Centrosomes. To determine whether the high centrosome number is associated with reduced growth in Lsh-deficient cells, we examined the ability of MEFs to incorporate BrdUrd, a marker for the S phase of the cell cycle. BrdUrd incorporation in

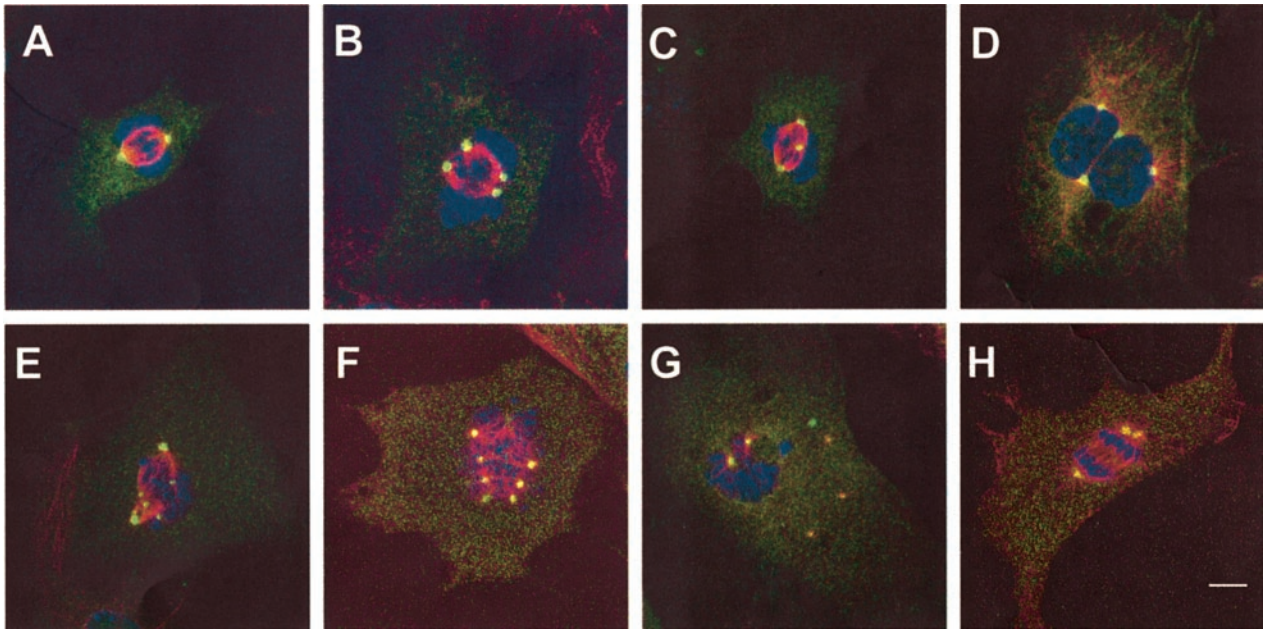

Fig. 4. Abnormal spindle formation in *Lsh*$^{-/-}$ MEF cultures. Wild-type MEFs (*A*) or *Lsh*$^{-/-}$ MEFs (*B–H*) were treated with 10 μM nocodazole for 20 h, then released in drug-free culture medium for 60–90 min and costained with anti-α-tubulin antibody (rhodamine-conjugated, *red*), antipericentrin-antibody (FITC-conjugated, *green*), and counterstained with (DAPI, *blue*). A wild-type mitotic cell contains two centrosome with bipolar spindle. *B–F* are *Lsh*$^{-/-}$ MEFs with abnormal spindle formation. *G*, *Lsh*$^{-/-}$ MEFs with cytoplasmic centrosomes that do not nucleate spindles. *H*, *Lsh*$^{-/-}$ MEFs with clustering of two centrosomes at one spindle pole and bipolar spindle formation. *Scale bar*, 10 μM.

Lsh$^{-/-}$ cells was reduced by ~50% in comparison with wild-type controls (data not shown), consistent with the results of tritium incorporation (Fig. 1*C*). Among BrdUrd-positive *Lsh*$^{-/-}$ cells, only ~12% cells had more than two centrosomes, whereas in the whole *Lsh*$^{-/-}$ population, ~25% of the cells contained more than two centrosomes. In addition, the relationship of cells with one *versus* two centrosomes was reversed in BrdUrd-positive *Lsh*$^{-/-}$ cells and equaled more closely the ratio in wild-type cells (33–45% in the whole *Lsh*$^{-/-}$ population *versus* 54 and 34% in the BrdUrd-positive population). Thus, the failure of Lsh-deficient cells to grow in culture is closely associated with abnormal centrosome numbers. These findings are consistent with a model in which defects in cell cycle division caused by absence of Lsh lead to subsequent accumulation of supernumerary centrosomes (as discussed below).

MEFs Treated with 5-aza-dC Show an Increase in Centrosome Numbers. We found substantial demethylation in *Lsh*$^{-/-}$ mice, including hypomethylation of repetitive elements that are usually highly methylated in wild-type cells (13). The level of hypomethylation in *Lsh*$^{-/-}$ MEF cultures was stable and did not change over many passages (P 4–P 30, data not shown). To test the idea whether genomic hypomethylation in Lsh-deficient cells may contribute to mitotic defects, wild-type MEF cells were treated with the demethylating drug 5-aza-dC. Genomic DNA was then analyzed for susceptibility to *Hpa*II digestion, a restriction enzyme that is highly methylation sensitive. As shown in Fig. 6*A*, *Lsh*$^{-/-}$ MEFs are greatly hypomethylated at minor satellite sequences that are located around centromeres in comparison to wild-type cells. Treatment with 5-aza-dC increased *Hpa*II digestibility in wild-type MEFs, indicating a decrease in methylation. This demethylation correlated with an increase in abnormal centrosome numbers (Fig. 6*B*). Wild-type MEFs displayed a 10-fold increase in the fraction of cells with abnormal centrosome numbers (raising from 4 to 35% after demethylation). *Lsh*$^{-/-}$ MEFs showed a rather modest increase of centrosome amplification of <2-fold (from 25 to 43%), consistent with the substantial hypomethylation observed in Lsh-deficient cells before drug treatment. The increase in centrosome numbers after demethylating treatment may be a characteristic of primary cells because demethylation of NIH3T3 cells did not lead to a significant increase of abnormal centrosome numbers (data not shown). Thus, hypomethylation by 5-aza-dC treatment could mimic the effect of Lsh deletion in embryonal fibroblasts.

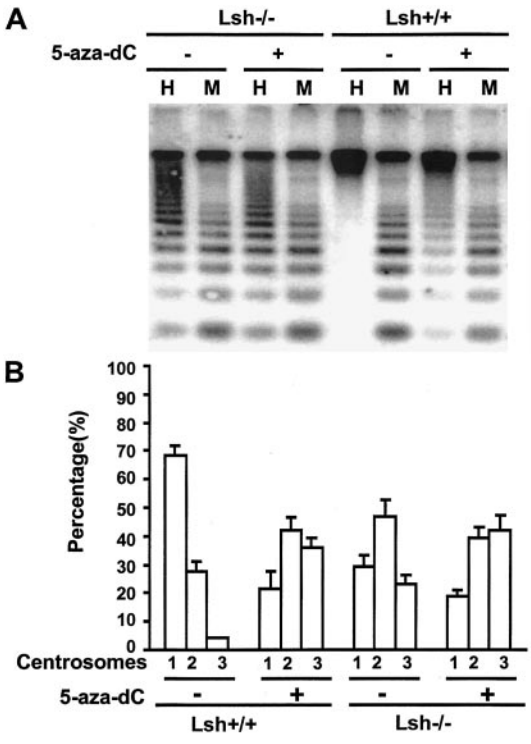

Fig. 6. Supernumerary centrosomes after genome demethylation. *A*, hypomethylation at minor satellite sequences. Wild-type and *LSH*$^{-/-}$ MEFs were cultured with and without 2.5 μM 5-aza-dC. Southern analysis was performed with methylation sensitive restriction enzyme *Hpa*II (H) or methylation-insensitive enzyme *Msp*I (M) and the blot probed for minor satellite sequences. *B*, MEFs were demethylated as described in *A* and then stained with antipericentrin antibodies to detect centrosomes. More than 500 cells were counted in one experiment for each group, and data are shown as the mean ± SD of three independent experiments.

DISCUSSION

Here, we demonstrate that the absence of Lsh leads to reduced growth of embryonal fibroblasts with signs of abnormal mitosis and increased numbers of centrosomes. Treatment of wild-type MEFs with a DNA demethylating drug results in a similar increase in centrosome numbers, suggesting that DNA hypomethylation plays an important role in the generation of mitotic defects in Lsh-deficient cells. Supernumerary functional centrosomes can lead to multipolar spindles and abnormal chromosome segregation as observed in Lsh mutant cells (17, 18, 23–26). Because global hypomethylation as well as centrosome amplification are frequently associated with cancer cells (3, 4), these findings suggest a novel link for genomic instability in cancer cells and a potential role for Lsh in tumor development.

The reduced growth rate of Lsh-deficient MEFs leads to a disadvantage in cellular transformation *in vitro*. This selective disadvantage appears to be in contrast with the suggested role of Lsh in tumor development based on an increase in centrosome numbers. A similar contradictory phenotype with reduced growth rate and abnormal centrosome numbers causing genomic instability has been observed in MEFs with a deletion of the breast cancer genes BRCA1 or BRCA2 (18, 19). Cells with supernumerary centrosomes are frequently forming multipolar spindles leading to arrest in cell division, mitotic catastrophes, and eventual to disappearance of these cells (23, 24, 26). How can these cells escape? The mitotic instability may on occasion lead to other genetic changes that are favorable for clonal expansion *in vivo* (26). For example, the loss of p53 and pRB checkpoints may allow to escape from cell cycle arrest caused by tetraploidy (25). In some cells, inactivation of extra centrosomes may occur or centrosome clustering (coalescence) allowing the cells to perform bipolar cell division despite the extra centrosomes (23, 24). In addition, it has been speculated that centrosome-independent spindle formation may arise (26).

How does Lsh deficiency or genomic hypomethylation give rise to supernumerary centrosomes? Distinct mechanisms for amplification of centrosomes have been suggested (19, 26): ranging from deregulation of the centrosome duplication cycle to rather indirect mechanism of mitotic failure leading to subsequent rounds of centrosome amplification. Currently, we do not have any evidence that Lsh (or DNA hypomethylation) plays any direct role in the centrosome duplication pathway. The activation of Cdk2 is thought to be a crucial regulator for centrosome duplication. We have not found any direct or indirect evidence for activation of this Cdk2 pathway: neither RB, E2F2, cyclin A, cyclin E protein levels, nor Cdk2 kinase activity (data not shown) were changed, and the p53 pathway (influencing Cdk2 activity) appeared unaffected (*e.g.*, unaltered p53 and p21 protein levels in Fig. 2*A* and cell cycle arrest and annexin staining after γ radiation was indistinguishable between wild-type and *Lsh*$^{-/-}$ MEFs; data not shown). An alternative pathway for increased centrosome numbers is mitotic failure subsequently leading to accumulation of centrosomes We hypothesize that the latter is the case in Lsh-deficient

cells and that possibly altered chromosome structure because of loss of Lsh may play a role in disturbed cell cycle progression. Lsh colocalizes to pericentromeric heterochromatin and alters DNA methylation and histone methylation levels at centromeric heterochromatin.[4] Because centromeric regions of chromosomes are important structures to ensure normal kinetochore formation, spindle fiber attachment, sister chromatid cohesion, and proper chromosome segregation, we hypothesize that disturbed centromeric chromosome structure in the absence of Lsh may contribute to cellular growth defects. This, in turn, may lead to subsequent accumulation of supernumerary centrosomes.

Epigenetic changes are thought to contribute to oncogenesis. Most hematopoietic and many solid tumors show signs of altered methylation patterns with genomic instability. Much focus has been on aberrant hypermethylation of promoter CpG islands that lead to silencing of tumor suppressor genes (2–4). Recent evidence demonstrates no correlation between hypermethylation and hypomethylation in Wilms' tumors, suggesting that DNA hypomethylation may contribute independently to cancer formation or tumor progression (30). Opposing effects of genomic hypomethylation on cancerogenesis have been reported, either promoting lymphoid tumors in mismatch repair-deficient mice or protecting against gastrointestinal tumor formation in APC/Min mutant mice (31–33). Furthermore, global hypomethylation in Dnmt1-deficient ES cells exhibited augmented mutation rates at endogenous loci because of genetic deletions and rearrangements (34). Thus, genomic hypomethylation may affect different pathways leading to genomic instability. Our data proposes a novel link by which deficiency of Lsh, a regulator of DNA methylation, leads to growth defects, abnormal mitosis with centrosome abnormalities that may promote genomic destabilization, and enhance the risk for cancer, a hypothesis that awaits additional testing in cancer models.

ACKNOWLEDGMENTS

We thank Drs. Joost Oppenheim, Ira Daar, and Nancy Colburn for critical comments on the manuscript. We also thank Terry Stull and Rodney Wiles for excellent technical assistance. We thank Dr. Sam Benchimol for the generous gift of the SV40 large T antigen.

REFERENCES

1. Bird, A. DNA methylation patterns and epigenetic memory. Genes Dev., *16:* 6–21, 2002.
2. Baylin, S., and Bestor, T. H. Altered methylation patterns in cancer cell genomes: cause or consequence? Cancer Cell, *1:* 299–305, 2002.
3. Feinberg, A. P. DNA methylation, genomic imprinting and cancer. Curr. Top. Microbiol. Immunol., *249:* 87–99, 2000.
4. Laird, P. W., and Jaenisch, R. The role of DNA methylation in cancer genetic and epigenetics. Annu. Rev. Genet., *30:* 441–464, 1996.
5. Meehan, R. R., and Stancheva, I. DNA methylation and control of gene expression in vertebrate development. Essays Biochem., *37:* 59–70, 2001.
6. Muchardt, C., and Yaniv, M. When the SWI/SNF complex remodels. the cell cycle. Oncogene, *20:* 3067–3075, 2001.
7. Gibbons, R. J., McDowell, T. L., Raman, S., O'Rourke, D. M., Garrick, D., Ayyub, H., and Higgs, D. R. Mutations in ATRX, encoding a SWI/SNF-like protein, cause diverse changes in the pattern of DNA methylation. Nat. Genet., *24:* 368–371, 2000.
8. Jeddeloh, J. A., Stokes, T. L., and Richards, E. J. Maintenance of genomic methylation requires a SWI2/SNF2-like protein. Nat. Genet., *22:* 94–97, 1999.
9. Jarvis, C. D., Geiman, T., Vila-Storm, M. P., Osipovich, O., Akella, U., Candeias, S., Nathan, I., Durum, S. K., and Muegge, K. A novel putative helicase produced in early murine lymphocytes. Gene (Amst.), *169:* 203–207, 1996.
10. Geiman, T. M., Durum, S. K., and Muegge, K. Characterization of gene expression, genomic structure, and chromosomal localization of Hells (Lsh). Genomics, *54:* 477–483, 1998.
11. Lee, D. W., Zhang, K., Ning, Z. Q., Raabe, E. H., Tintner, S., Wieland, R., Wilkins, B. J., Kim, J. M., Blough, R. I., and Arceci, R. J. Proliferation-associated SNF2-like gene (PASG): a SNF2 family member altered in leukemia. Cancer Res., *60:* 3612–3622, 2000.
12. Geiman, T. M., Tessarollo, L., Anver, M. R., Kopp, J. B., Ward, J. M., and Muegge, K. Lsh, a SNF2 family member, is required for normal murine development. Biochim. Biophys. Acta, *1526:* 211–220, 2001.
13. Dennis, K., Fan, T., Geiman, T., Yan, Q., and Muegge, K. Lsh, a member of the SNF2 family, is required for genome-wide methylation. Genes Dev., *15:* 2940–2944, 2001.
14. Selker, E. U. Trichostatin A causes selective loss of DNA methylation in Neurospora. Proc. Natl. Acad. Sci. USA, *95:* 9430–9435, 1998.
15. Tamaru, H., and Selker, E. U. A histone H3 methyltransferase controls DNA methylation in Neurospora crassa. Nature (Lond.), *414:* 277–283, 2001.
16. Geiman, T. M., and Muegge, K. Lsh, an SNF2/helicase family member, is required for proliferation of mature T lymphocytes. Proc. Natl. Acad. Sci. USA, *97:* 4772–4777, 2000.
17. Marx, J. Cell biology. Do centrosome abnormalities lead to cancer? Science (Wash. DC), *292:* 426–429, 2001.
18. Kramer, A., and Ho, A. D. Centrosome aberrations and cancer. Onkologie, *24:* 538–544, 2001.
19. Meraldi, P., and Nigg, E. A. The centrosome cycle. FEBS Lett., *521:* 9–13, 2002.
20. Todaro, G. J., and Green, H. Quantitative studies of the growth of mouse embryo cells in cultures and their development into established lines. J. Cell Biol., *17:* 299–313, 1963.
21. McAuliffe, M. J., Lalonde, F. M., McGarry, D., Gandler, W., Csaky, K., and Trus, B. L. Medical image processing, analysis, and visualization in clinical research. IEEE Computer-Based Medical Systems, 2001.
22. Kim, H., You, S., Farris, J., Kong, B. W., Christman, S. A., Foster, L. K., and Foster, D. N. Expression profiles of p53-, p16(INK4a)-, and telomere-regulating genes in replicative senescent primary human, mouse, and chicken fibroblast cells. Exp. Cell Res., *272:* 199–208, 2002.
23. Salisbury, J. L., Whitehead, C. M., Lingle, W. L., and Barrett, S. L. Centrosomes and cancer. Biol. Cell, *91:* 451–460, 1999.
24. Brinkley, B. R. Managing the centrosome numbers game: from chaos to stability in cancer cell division. Trends Cell Biol., *11:* 18–21, 2001.
25. Margolis, R. L., Lohez, O. D., and Andreassen, P. R. G_1 tetraploidy checkpoint and the suppression of tumorigenesis. J. Cell. Biochem., *88:* 673–683, 2003.
26. Nigg, E. A. Centrosome aberrations: cause or consequence of cancer progression? Nat. Rev. Cancer, *2:* 815–825, 2002.
27. Borel, F., Lohez, O. D., Lacroix, F. B., and Margolis, R. L. Multiple centrosomes arise from tetraploidy checkpoint failure and mitotic centrosome clusters in p53 and RB pocket protein-compromised cells. Proc. Natl. Acad. Sci. USA, *99:* 9819–9824, 2002.
28. Xu, X., Weaver, Z., Linke, S. P., Li, C., Gotay, J., Wang, X. W., Harris, C. C., Ried, T., and Deng, C. X. Centrosome amplification and a defective G_2-M cell cycle checkpoint induce genetic instability in BRCA1 exon 11 isoform-deficient cells. Mol. Cell, *3:* 389–395, 1999.
29. Tutt, A., Gabriel, A., Bertwistle, D., Connor, F., Paterson, H., Peacock, J., Ross, G., and Ashworth, A. Absence of Brca2 causes genome instability by chromosome breakage and loss associated with centrosome amplification. Curr. Biol., *9:* 1107–1110, 1999.
30. Ehrlich, M., Jiang, G., Fiala, E., Dome, J. S., Yu, M. C., Long, T. I., Youn, B., Sohn, O. S., Widschwendter, M., Tomlinson, G. E., Chintagumpala, M., Champagne, M., Parham, D., Liang, G., Malik, K., and Laird, P. W. Hypomethylation and hypermethylation of DNA in Wilms' tumors. Oncogene, *21:* 6694–6702, 2002.
31. Trinh, B. N., Long, T. I., Nickel, A. E., Shibata, D., and Laird, P. W. DNA methyltransferase deficiency modifies cancer susceptibility in mice lacking DNA mismatch repair. Mol. Cell. Biol., *22:* 2906–2917, 2002.
32. Laird, P. W., Jackson-Grusby, L., Fazeli, A., Dickinson, S. L., Jung, W. E., Li, E., Weinberg, R. A., and Jaenisch, R. Suppression of intestinal neoplasia by DNA hypomethylation. Cell, *81:* 197–205, 1995.
33. Eads, C. A., Nickel, A. E., and Laird, P. W. Complete genetic suppression of polyp formation and reduction of CpG-island hypermethylation in Apc(Min/+) Dnmt1-hypomorphic Mice. Cancer Res., *62:* 1296–1299, 2002.
34. Chen, R. Z., Pettersson, U., Beard, C., Jackson-Grusby, L., and Jaenisch, R. DNA hypomethylation leads to elevated mutation rates. Nature (Lond.), *395:* 89–93, 1998.

[4] Q. Yan, J. Huang, T. Fan, S. Lockett, and K. Muegge, unpublished observations.